Target of rapamycin signaling mediates vacuolar fission caused by endoplasmic reticulum stress in *Saccharomyces cerevisiae*

Bobbiejane Stauffer and Ted Powers
Department of Molecular and Cellular Biology, College of Biological Sciences, University of California, Davis, Davis, CA 95616

ABSTRACT **The yeast vacuole is equivalent to the mammalian lysosome and, in response to diverse physiological and environmental stimuli, undergoes alterations both in size and number. Here we demonstrate that vacuoles fragment in response to stress within the endoplasmic reticulum (ER) caused by chemical or genetic perturbations. We establish that this response does not involve known signaling pathways linked previously to ER stress but instead requires the rapamycin-sensitive TOR Complex 1 (TORC1), a master regulator of cell growth, together with its downstream effectors, Tap42/Sit4 and Sch9. To identify additional factors required for ER stress–induced vacuolar fragmentation, we conducted a high-throughput, genome-wide visual screen for yeast mutants that are refractory to ER stress–induced changes in vacuolar morphology. We identified several genes shown previously to be required for vacuolar fusion and/or fission, validating the utility of this approach. We also identified a number of new components important for fragmentation, including a set of proteins involved in assembly of the V-ATPase. Remarkably, we find that one of these, Vph2, undergoes a change in intracellular localization in response to ER stress and, moreover, in a manner that requires TORC1 activity. Together these results reveal a new role for TORC1 in the regulation of vacuolar behavior.**

Monitoring Editor
Reid Gilmore
University of Massachusetts

Received: Jun 8, 2015
Revised: Sep 14, 2015
Accepted: Oct 7, 2015

INTRODUCTION

The endoplasmic reticulum (ER) lumen provides an environment for newly synthesized secretory proteins to fold properly and undergo posttranslational modifications to achieve their final native functional conformation. Disruption of protein folding can result in accumulation of unfolded proteins in the ER lumen that overwhelms its normal folding capacity, a condition characterized as ER stress. ER stress can be initiated by various circumstances, including overexpression of secretory proteins, inhibition of protein glycosylation, and change in redox state (Spear and Ng, 2003). Transduction of ER stress is signaled predominantly by the unfolded protein response (UPR), which works to restore ER homeostasis by simultaneously reducing protein load and increasing folding capacity within the ER (Walter and Ron, 2011). Alternative ER stress pathways have also been identified, including the ER surveillance pathway (ERSU), which delays ER inheritance until ER stress is resolved (Babour *et al.*, 2010), and ER-associated degradation (ERAD), which retrotranslocates unfolded or misfolded proteins from the ER to the cytosol for proteasomal-targeted degradation (McCracken *et al.*, 1996). Furthermore, the ER membrane can undergo expansion according to cellular need via increased lipid biosynthesis, a process mediated by the Ino2/4 transcription factor complex (Schuck *et al.*, 2009).

ER stress elicits diverse and complex cellular responses, including intracellular signaling and changes in gene expression, and can stimulate both autophagy and apoptosis (Rutkowski and Kaufman, 2004). For example, the UPR induces Ire1-dependent splicing of Hac1 mRNA to form an active transcription factor that enters the nucleus to increase expression of genes involved in lipid metabolism, cell wall biogenesis, and vesicular trafficking (Travers *et al.*, 2000). In addition, the effect of ER stress extends to regulation of

This article was published online ahead of print in MBoC in Press (http://www.molbiolcell.org/cgi/doi/10.1091/mbc.E15-06-0344) on October 14, 2015.

Address correspondence to: Ted Powers (tpowers@ucdavis.edu).

Abbreviations used: CHX, cycloheximide; DMSO, dimethyl sulfoxide; DTT, dithiothreitol; ER, endoplasmic reticulum; ERAD, ER-associated degradation; ERSU, ER stress surveillance; PI(3,5)P_2, phosphatidylinositol 3,5 bisphosphate; Rap, rapamycin; Tm, tunicamycin; TORC1, target of rapamycin complex 1; UPR, unfolded protein response.

the vacuole, where it was reported that tunicamycin (Tm), a drug that induces ER stress by inhibition of N-linked glycosylation, results in changes in vacuolar morphology by inducing vacuolar fragmentation (Kim *et al.*, 2012). Remarkably, the influence of ER stress on vacuolar structure and function has remained largely unexplored.

The yeast vacuole is analogous to the mammalian lysosome and functions in processes required for cellular homeostasis, including protein degradation, nutrient storage, and maintenance of cytoplasmic pH (Weisman, 2003). Vacuolar morphology is regulated by the equilibrium between vacuolar fusion and fission activities (Baars *et al.*, 2007; Li and Kane, 2009). Under normal growth conditions, wild-type (WT) cells typically possess between one and four vacuoles, depending on the strain background (Banta *et al.*, 1988). The balance between fusion and fission underlies the ability of vacuoles to rapidly alter their morphology in response to environmental conditions—for example, coalescing to form a single large vacuole under nutrient limitation versus fragmenting into numerous smaller vacuoles in response to hyperosmotic shock (Baba *et al.*, 1994; Bonangelino *et al.*, 2002). Vacuolar fragmentation also occurs during cell cycle progression, where smaller vacuoles are partitioned for proper inheritance into the daughter cell (Weisman, 2003). In both of these examples, fragmentation relies on increased levels of phosphatidylinositol 3,5-bisphosphate ($PI(3,5)P_2$), a lipid that is enriched at the vacuole (Dove *et al.*, 1997, 2002; Bonangelino *et al.*, 2002; Weisman, 2003). By contrast, a requirement for other fragmentation factors may depend on the specific inducing stimuli (Bonangelino *et al.*, 2002; Zieger and Mayer, 2012). For example, both the dynamin-like protein Vps1 and the vacuolar ATPase (V-ATPase) are required for osmotic stress–induced vacuolar fragmentation yet appear to be dispensable for fragmentation during cell cycle progression (Zieger and Mayer, 2012). Thus, whereas vacuolar fusion has been studied extensively and many of the required components have been identified and characterized, vacuole fission remains poorly understood.

Prior studies have revealed a role for target of rapamycin complex 1 (TORC1) in vacuolar fission during hyperosmotic stress (Michaillat *et al.*, 2012). The TOR signaling network is a highly conserved regulator of cell growth that consists of two distinct protein complexes, TORC1 and TORC2, where TORC1 is uniquely inhibited by the macrolide drug rapamycin (Loewith and Hall, 2011). The Tor1 and Tor2 kinases form the catalytic component of these protein complexes (Loewith and Hall, 2011). TORC1 is composed of Tor1 or Tor2, Tco89, Kog1, and Lst8 and is enriched at the vacuolar membrane (Urban *et al.*, 2007; Sturgill *et al.*, 2008), where it regulates diverse cellular processes in response to both nutrient and stress conditions (Urban *et al.*, 2007; Binda *et al.*, 2009; Loewith and Hall, 2011). Rapamycin treatment or deletion of the nonessential TORC1-specific component Tco89 results in inhibition of vacuolar fragmentation after hyperosmotic stress (Michaillat *et al.*, 2012). By contrast, to date a role for TORC1 in ER stress-induced fragmentation has not been examined. Accordingly, in this study, we demonstrate a role for TORC1 in ER stress–induced vacuolar fragmentation. Furthermore, we carried out a forward genetic screen and identified several additional factors required for vacuolar fragmentation in response to ER stress.

RESULTS

Examination of vacuolar morphology during ER stress

Results of a previous study demonstrated that in the presence of tunicamycin, WT cells contain fragmented vacuoles (Kim *et al.*, 2012). To confirm these findings and determine whether this change in vacuolar morphology resulted strictly from Tm treatment or was a result of general ER stress, we examined vacuolar structure after treatment of cells with either Tm or dithiothreitol (DTT), a reducing agent that prevents disulfide bond formation and is an independent inducer of ER stress (Cox *et al.*, 1993; Jamsa *et al.*, 1994). The number of vacuoles per cell was counted, and cells containing five or more vacuoles were scored as fragmented, as previously described (Michaillat *et al.*, 2012). Unstressed cells contained primarily a single vacuole per cell (Figure 1A). As expected, a majority of cells treated with Tm displayed smaller and more numerous vacuoles, indicative of fragmentation (Figure 1A). Similarly, the number of cells with fragmented vacuoles increased significantly upon treatment with DTT (Figure 1A). The degree of fragmentation in DTT-treated cells was not as extensive as that seen with Tm, consistent with reports that reducing agents are not as robust an inducer of the UPR (Cox *et al.*, 1993; Bonilla *et al.*, 2002).

The kinetics of vacuolar fragmentation appeared similar to that of Hac1 mRNA splicing, a hallmark of UPR induction, for which maximum induction occurs at ~2 h of treatment (Bicknell *et al.*, 2010). In addition, we observed that re-formation of fewer and larger vacuoles after removal of Tm from cells required ~7 h of growth in fresh medium (Supplemental Figure S1). Given that at least 4 h is required for ER stress to become resolved after removal of Tm (Bicknell *et al.*, 2010), we conclude that vacuolar fragmentation both follows resolution of ER stress and requires conditions for new cell growth.

To extend these results and confirm that vacuolar fragmentation was not caused by off-target or nonspecific effects of Tm and/or DTT, we used a genetic approach to induce ER stress. Specifically, we examined the role of *ERO1*, encoding endoplasmic reticulum oxidoreductin 1, which catalyzes disulfide bond formation and isomerization within the ER, by inactivation of the temperature-sensitive *ero1-1* allele (Frand and Kaiser, 1998). We observed that vacuolar morphology was normal in *ero1-1* cells grown at the permissive temperature of 25°C but that vacuoles became fragmented when these cells were shifted to the nonpermissive temperature of 37°C (Figure 1B). The kinetics of fragmentation was very similar to that observed using the chemical inducers, for which maximal effects were observed ~2 h after the temperature shift. Together these results indicate that vacuolar fragmentation correlates with ER stress, as defined by Tm and DTT treatment and *ERO1* inactivation.

Vacuolar fragmentation is independent of known ER stress response pathways

To understand how ER stress influences vacuolar morphology, we assessed whether known pathways that are induced upon ER stress are involved in vacuolar fragmentation. We first tested whether the UPR was required for this response, which in yeast is initiated by the transmembrane kinase and endoribonuclease Ire1 (Sidrauski and Walter, 1997; Okamura *et al.*, 2000). Accordingly, we examined vacuolar morphology in cells lacking Ire1 after Tm treatment, for which we observed that vacuoles in *ire1Δ* cells underwent fragmentation to the same extent as in WT cells (Figure 2A and Supplemental Figure S2A), indicating that the UPR is not required for vacuolar fragmentation.

We next tested the ERSU pathway, which functions independently of the UPR through the MAP kinase Slt2 (Mpk1) to delay ER inheritance during ER stress (Babour *et al.*, 2010). Specifically, we analyzed vacuolar morphology in *slt2Δ* cells after Tm treatment and observed that vacuolar fragmentation in *slt2Δ* cells was comparable to that for WT (Figure 2B and Supplemental Figure S2B), indicating that ERSU is also not involved in this process.

We next examined involvement of ERAD, which requires the E3 ubiquitin ligase Hrd1 to ubiquitinate ERAD substrates and target

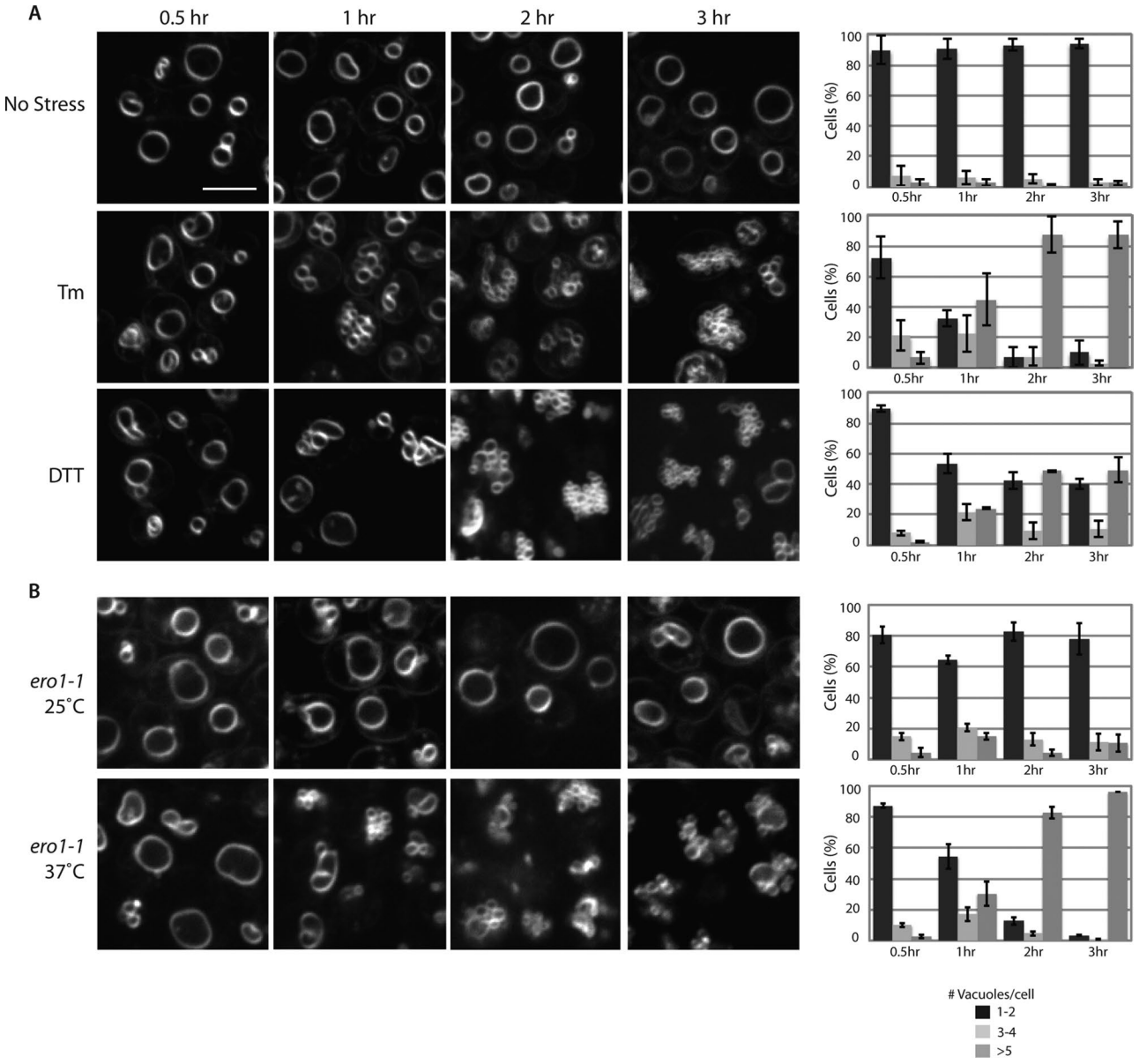

FIGURE 1: ER stress results in vacuolar fragmentation. (A) WT (W303α) or *ero1*-1 cells were grown overnight at 30 and 25°C, respectively, to early log phase in YPD + 1 μM FM4-64. WT cells were then treated with DMSO (No Stress), 1 μg/ml Tm, or 25 μM DTT. (B) The *ero1-1* cells either remained at 25°C or were centrifuged and resuspended in 37°C YPD and incubated at 37°C for the indicated times. Cells were centrifuged and immediately visualized using fluorescence microscopy (spinning-disk confocal; Intelligent Imaging Innovations). Scale bar, 5 μm. The number of vacuoles per cell was counted (100 cells/condition) and categorized into one of three groups. The averages of three independent experiments are presented ± SEM.

them for degradation (Bays *et al.*, 2001; Deak and Wolf, 2001; Swanson *et al.*, 2001). We observed that vacuoles in *hrd1Δ* cells underwent vacuolar fragmentation to the same extent as in WT after treatment with Tm (Figure 2C and Supplemental Figure S2B), excluding as well the involvement of ERAD in the regulation of vacuolar morphology.

Finally, we tested involvement of ER membrane expansion that occurs in response to ER stress, which accommodates an increased load of unfolded proteins. This expansion relies in part on the Ino2/4 transcription factor complex, which targets lipid biosynthetic genes (Schuck *et al.*, 2009). We examined the ability of vacuoles to fragment when membrane expansion was blocked by deletion of INO4. We observed that *ino4Δ* cells displayed fragmented vacuoles after ER stress, excluding this response as well (Figure 2D and Supplemental Figure S2B). Together these data suggest that vacuolar morphology is regulated by ER stress via components that are distinct from known regulators of ER homeostasis.

Demonstrating a role for TORC1 in ER stress–mediated vacuolar fragmentation

Previous studies implicated TORC1 as a positive regulator of vacuolar fragmentation in response to hyperosmotic shock (Michaillat *et al.*, 2012). Furthermore, rapamycin treatment inhibits TORC1 and promotes coalescence of vacuoles into a single large organelle (Cardenas and Heitman, 1995; Dubouloz *et al.*, 2005; Michaillat *et al.*, 2012). Accordingly, we tested whether TORC1 was required

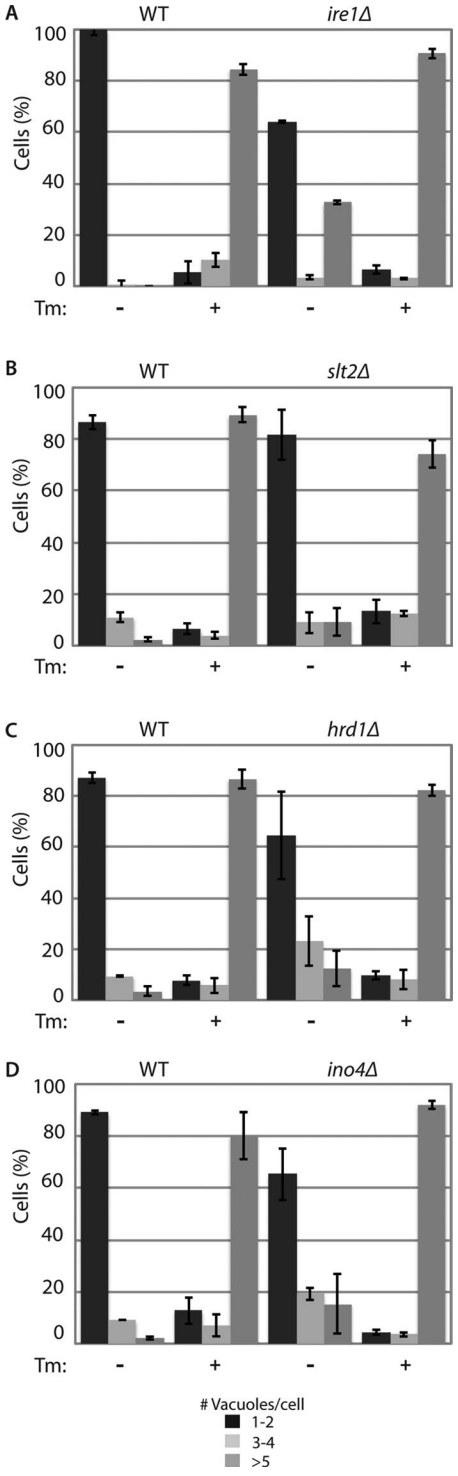

FIGURE 2: Tm-induced vacuolar fission occurs independently of known ER stress response pathways. (A) *ire1Δ* (PLY1637) and isogenic WT (W303α) cells were grown at 30°C overnight in YPD + 1 μM FM4-64 to OD_{600} = 0.25 and then treated with DMSO or 1 μg/ml Tm for 2 h. Cells were centrifuged and immediately visualized using fluorescence microscopy. Vacuolar morphology was quantified as described in Figure 1. The average of three independent experiments is shown ± SEM. (B–D) WT (BY4741), *slt2Δ*, *hrd1Δ*, and *ino4Δ* cells were grown and analyzed as in A.

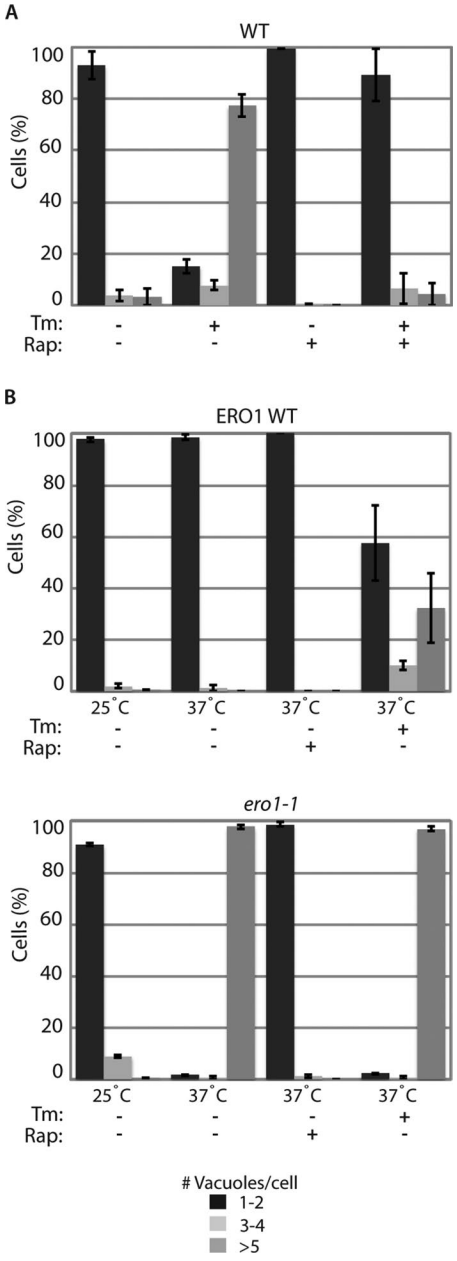

FIGURE 3: TORC1 is required for Tm-induced vacuolar fragmentation. (A) WT (W303α) cells were grown overnight as described in Figure 1. Cells were treated with DMSO, 1 μg/ml Tm, 200 nM Rap, or both 1 μg/ml Tm and 200 nM Rap for 2 h, then centrifuged and immediately visualized using fluorescence microscopy. Quantification of vacuolar morphology was performed as described in Figure 1. (B) ERO1 and *ero1-1* cells were grown at 25°C overnight in YPD + 1μM FM4-64 to OD_{600} = 0.25. Cells either remained at 25°C or were centrifuged and resuspended in 37°C YPD with either 200 nM Rap or 1 μg/ml Tm.

for ER stress–induced vacuolar fragmentation by simultaneously treating cells with Tm to induce ER stress, as well as with rapamycin, and analyzed vacuolar morphology. As expected, WT cells treated with Tm contained fragmented vacuoles, whereas cells treated with rapamycin maintained a single large vacuole (Figure 3A and Supplemental Figure S3A). Of importance, fragmentation induced by Tm was blocked when TORC1 was inhibited by rapamycin, suggesting that TORC1 activity is required for ER stress–induced vacuolar fragmentation (Figure 3A and Supplemental Figure S3A). Moreover, rapamycin treatment also blocked vacuolar fragmentation in temperature-shifted *ero1-1* cells, confirming the dependence of fragmentation on TORC1 activity (Figure 3B).

Prior studies showed that TORC1 functions through at least two major downstream effector branches, defined by the proteins Tap42 and Sch9, to regulate a diverse array of cellular processes (Di Como and Arndt, 1996; Duvel *et al.*, 2003; Urban *et al.*, 2007). We therefore tested whether either of these branches was required for vacuolar fragmentation. Because TAP42 is encoded by an essential gene, we used a temperature-sensitive allele, termed *tap42-106* (Duvel *et al.*, 2003), to examine vacuolar structure during ER stress at permissive versus nonpermissive temperatures. We observed that Tm-treated WT cells contained fragmented vacuoles at both the permissive temperature of 25°C and after a shift of cells to the nonpermissive temperature of 37°C (Figure 4A and Supplemental Figure S3B). By contrast, we observed that whereas *tap42-106* cells displayed fragmented vacuoles after Tm treatment at 25°C, vacuoles remained nonfragmented in response to Tm at 37°C (Figure 4A and Supplemental Figure S3B). These data indicate that the Tap42 branch of TORC1 is required for ER stress–induced vacuolar fragmentation. Tap42 has been proposed to interact with and regulate the activity of the type2A phosphatase Sit4 (Di Como and Arndt, 1996; Jiang and Broach, 1999). Therefore we examined whether fragmentation occurred in Sit4-deficient cells. On treatment with Tm, *sit4Δ* cells were unable to undergo vacuolar fragmentation, indicating that Sit4 activity is also required for Tm-induced vacuolar fragmentation (Figure 4B and Supplemental Figure S3C).

We next examined the role of Sch9 in vacuolar fragmentation during ER stress. Sch9 is an AGC kinase and a likely orthologue of mammalian (S6K1) and has been implicated in the regulation of several activities downstream of TORC1, including cellular responses to osmotic and oxidative stresses (Urban *et al.*, 2007). During Tm treatment, vacuolar fragmentation was blocked in *sch9Δ* cells (Figure 4C and Supplemental Figure S3C), suggesting that Sch9 is also required for vacuolar fragmentation in response to ER stress. These data suggest that both the Tap42 and Sch9 effector branches are required downstream of TORC1 for ER stress–induced vacuolar fragmentation.

Because TORC1 is localized to the vacuole, we sought to determine whether this localization changed during vacuolar fragmentation. Accordingly, we examined the localization of functional green fluorescent protein (GFP)–tagged versions of the TORC1-specific components Tor1 and Tco89 after Tm treatment. Colocalization of GFP signal to the vacuolar membrane, marked by FM4-64, was quantified as described in *Materials and Methods*. On ER stress, the majority of Tor1-GFP and Tco89-GFP (75 and 85%, respectively) remained localized to the vacuolar membrane (Figure 5) during vacuolar fragmentation. These findings suggest that TORC1 functions in vacuolar fission at the vacuolar membrane.

Exploring the relationship between TORC1 and ER stress

To characterize further the relationship between ER stress and TORC1, we asked whether TORC1 and ER stress function independently or, alternatively, together within a linear pathway to influence vacuolar morphology (Figure 6A). We reasoned that if ER stress functions upstream of TORC1, then Tm treatment might stimulate TORC1 activity, as proposed for activation of TORC1 by hyperosmotic stress (Michaillat *et al.*, 2012). Alternatively, a study reported that Tm treatment results in decreased TORC1 activity (Lempiainen *et al.*, 2009). Accordingly, we used a previously established gel mobility shift assay to examine the behavior of the TORC1 pathway–specific target Npr1, which functions downstream of Tap42 and is phosphorylated in a rapamycin-sensitive manner (Schmidt *et al.*, 1998; Gander *et al.*, 2008; Graef and Nunnari, 2011). As a positive control for detecting increased TORC1 activity, we treated cells with

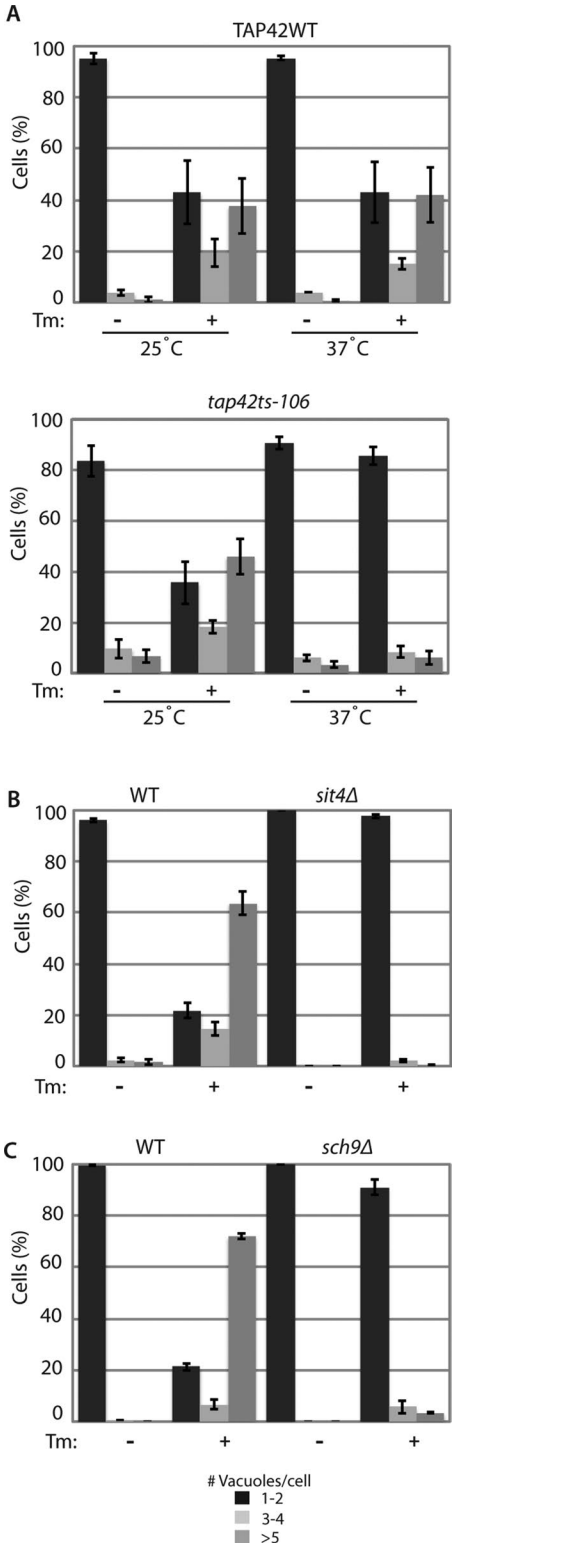

FIGURE 4: TORC1 effectors are required for Tm-induced vacuolar fragmentation. (A) TAP42WT (PLY553) and *tap42ts-106* (PLY551) were grown overnight in SCD –Trp + 1 μM FM4-64 medium to OD_{600} = 0.25 at 25°C. Cells were incubated at either 25 or 37°C for 30 min and then treated with DMSO or 1 μg/ml Tm for 2 h and visualized using fluorescence microscopy. Vacuolar morphology was quantified as described in Figure 1. (B, C) WT, *sit4Δ*, and *sch9Δ* (W303α, PLY1638, and PLY1639, respectively) cells were grown and treated, and vacuolar morphology was quantified as described in Figure 1.

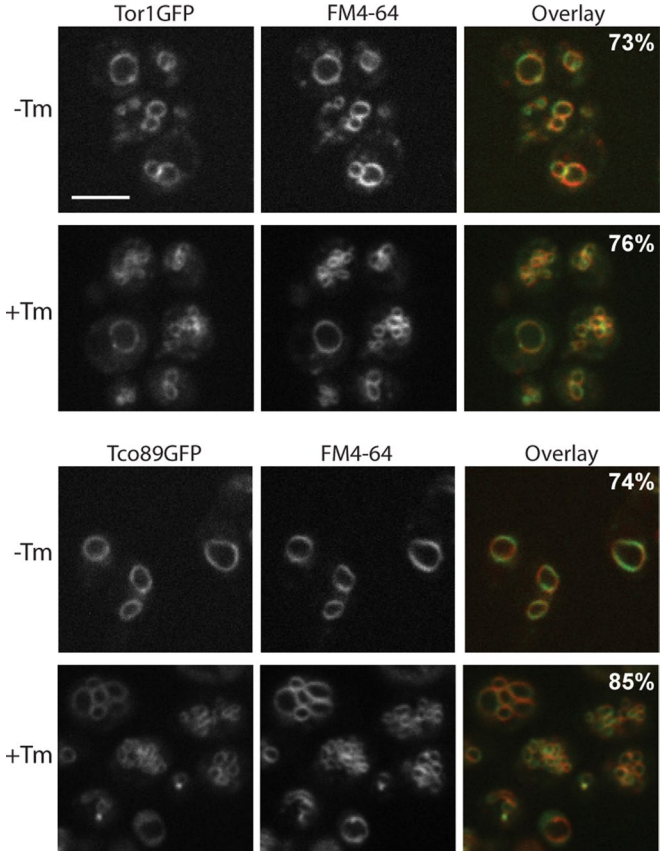

FIGURE 5: TORC1 remains localized to the vacuolar membrane upon vacuolar fragmentation. Tor1GFP (PLY1176) and Tco89GFP (PLY1640) cells were grown overnight at 30°C to early log phase (OD_{600} = 0.25) in YPD + 1μM FM4-64 medium. Cells were treated with DMSO or 1 μg/ml Tm for 2 h, and then live cells were imaged using the spinning disk confocal microscope (Intelligent Imaging Innovations). Percentages indicate colocalization of GFP to FM4-64 signal as determined using Imaris software. Scale bar, 5 μm.

sublethal doses of cycloheximide (CHX), a proposed activator of TORC1 (Beugnet *et al.*, 2003; Urban *et al.*, 2007). As expected, our results showed that Npr1 was both hyperphosphorylated after CHX treatment and dephosphorylated by rapamycin, confirming the utility of this assay (Figure 6B). By contrast, no significant change in the mobility of Npr1 was detected after treatment of cells with Tm throughout the same time period that coincided with maximal vacuolar fragmentation (Figure 6B).

To extend these results, we used a similar gel shift mobility assay to examine the phosphorylation state of Par32, a distinct target downstream of TORC1/Tap42 that instead becomes hyperphosphorylated upon inhibition of TORC1activity by rapamycin treatment (Huber *et al.*, 2009). As expected, we observed that Par32 mobility decreased after rapamycin treatment but saw no significant change in mobility after treatment with Tm (Figure 6C). Finally, we examined a third TORC1-dependent substrate, Atg13, which is directly phosphorylated by TORC1 at multiple serine residues (Kamada *et al.*, 2010). Again, we observed predicted changes in mobility after treatment with rapamycin and CHX but no change with Tm (Supplemental Figure S4). On the basis of these results, we conclude that ER stress does not affect TORC1 activity, as measured using these approaches. Accordingly, we conclude that TORC1 is likely to function in a pathway that is parallel to ER stress in order to regulate vacuolar fragmentation.

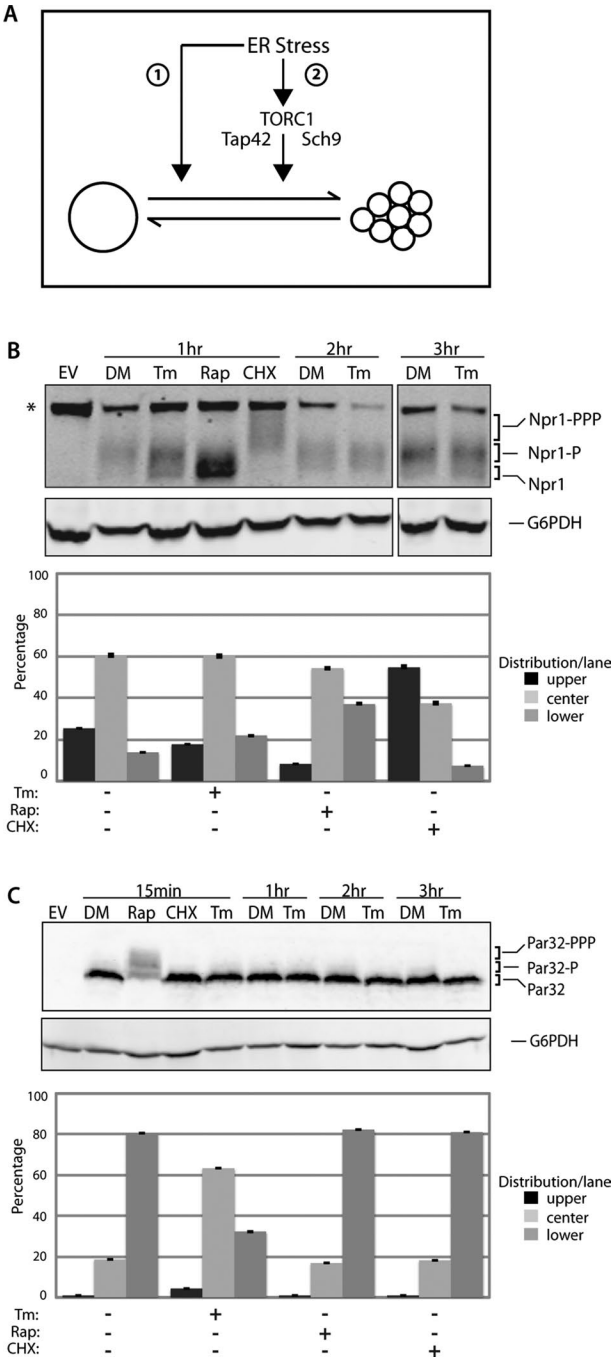

FIGURE 6: Evidence that ER stress and TORC1 are likely to act in parallel pathways to influence vacuolar morphology. (A) Model of vacuolar fragmentation depicting ER stress and TORC1 acting on vacuolar morphology in either (1) a parallel pathway or (2) a linear pathway. (B) Wild-type (W303α) cells expressing pr^{NPR1}-NPR1-HA were grown in SCD –Trp medium containing DMSO (DM), Tm (1 μg/ml), Rap (200 ng), or CHX (25 μg/ml). Cells were analyzed at indicated time points by whole-cell extraction and Western blot analysis using anti-HA and anti-G6PDH antibodies. Quantification of the relative distribution of signal per lane was performed by measuring the level of signal in each portion of the lane—upper (hyperphosphorylated), center (phosphorylated), and lower (dephosphorylated)—and dividing each portion by the total amount of signal in the lane. Averages of three independent experiments are presented ± SEM. (C) WT (W303α) cells expressing HA-tagged Par32 were grown, treated, and subjected to Western blot analysis as described in B. Relative distribution of signal per lane was quantified as described in B.

A

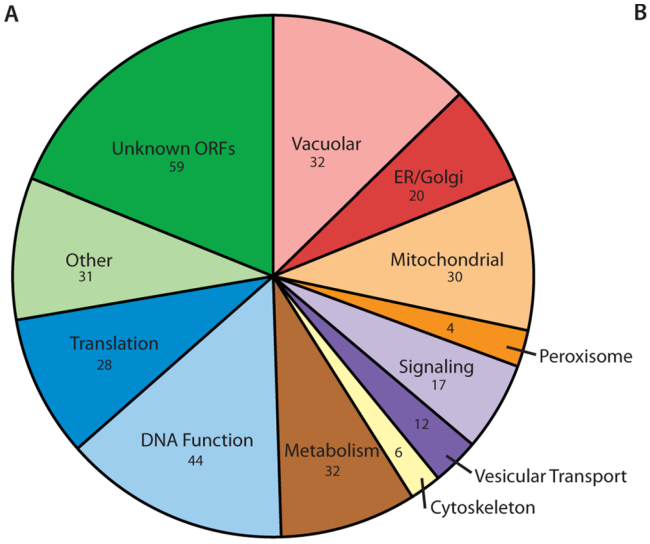

B

	# of vacuoles/cell (TM)		
ORF	1 to 2	3 to 4	>5
WT	11.7%	8.0%	80.3%
TOR Signaling			
sit4	60.8%	15.3%	23.9%
vps9	49.2%	23.4%	27.4%
V-ATPase (V0 Domain)			
vma6	90.5%	7.2%	2.3%
vma3	75.7%	13.7%	10.5%
vma16	69.9%	15.4%	14.7%
V-ATPase (V1 Domain)			
vma7	90.5%	9.5%	0.0%
vma8	50.7%	26.8%	22.6%
V-ATPase Assembly			
vph2	73.8%	3.3%	23.0%
vma21	73.8%	16.6%	9.6%
AP-3 Complex			
apl6	95.0%	5.0%	0.0%
apm3	90.1%	6.8%	3.2%
aps3	76.5%	11.0%	12.5%
apl5	46.0%	3.0%	51.0%
Trafficking			
atg8	76.0%	12.0%	12.0%
vps3	74.0%	15.0%	11.0%
pep12	70.3%	15.8%	13.9%
pep7	67.0%	15.6%	17.5%
PIP(3,5) Synthesis			
vps15	91.3%	3.3%	5.4%
fab1	79.6%	4.1%	16.3%
Other			
srb8	69.8%	11.3%	18.9%
cys4	56.3%	21.4%	22.4%
ypr099c	55.7%	25.7%	18.6%

FIGURE 7: Genome-wide screen elucidates genes required for Tm-induced vacuolar fragmentation. (A) Manually defined functional categorization of 315 genes found to have a defect in vacuolar fragmentation upon Tm treatment. (B) Quantification of yeast deletion strains with the strongest defects in vacuolar fragmentation upon Tm treatment. Genes are manually grouped according to function. Genes depicted in A are listed in Supplemental Table S1.

A number of components have been proposed to act upstream of TORC1 and regulate its activity in yeast, in particular proteins that comprise the EGO complex, including Ego1 and Ego3, as well as Gtr1 and Gtr3, orthologues of the mammalian Rag 1-4 GTPases, which regulate mTORC1 activity (Dubouloz *et al.*, 2005; Gao and Kaiser, 2006; Kim *et al.*, 2008; Sancak *et al.*, 2008; Binda *et al.*, 2009; Zhang *et al.*, 2012). Precisely how these proteins regulate TORC1 activity in yeast remains ill defined (Gao and Kaiser, 2006; Zhang *et al.*, 2012; Powis *et al.*, 2015). We examined the fragmentation behavior of mutants for each of these components and, unexpectedly, observed a variety of phenotypes (Supplemental Figure S5). For example, *ego3Δ* cells behaved most closely to what would be expected of a mutant within an upstream regulator of TORC1, where there was a strong block in vacuolar fragmentation after Tm treatment. By contrast, both *gtr1Δ* and *gtr2Δ* cells already displayed a significant number of cells that possessed fragmented vacuoles in the absence of Tm treatment and then became fully fragmented after drug treatment (Supplemental Figure S5). Finally, *ego1Δ* cells behaved like WT in that they displayed no fragmentation defect when treated with Tm (Supplemental Figure S5). We attribute this diversity in the response of these mutants to Tm to the complexity that likely exists in the upstream regulation of TORC1 in yeast.

Identification of factors required for ER stress–induced vacuolar fragmentation

To further our understanding of processes that control vacuolar fission, we sought to identify additional components involved in transduction of ER-derived stress signals to the vacuole. Therefore we carried out an in vivo visual screen of the haploid yeast deletion collection of nonessential genes to identify mutants that displayed defects in vacuolar fragmentation in response to treatment with Tm. After an initial screen of the entire collection (~5000 strains), mutants possessing at least 50% of cells with fragmentation defects were rearrayed and examined two additional times using high-throughput microscopy, where we included treatment with DTT in addition to Tm. Through this process, we identified 315 mutants that displayed reproducible fragmentation defects in response to ER stress (Figure 7A and Supplemental Table S1). Of these candidates, mutants with the strongest phenotypes (>70% cells containing nonfragmented vacuoles), along with 14 additional positive candidates involved in cellular signaling, were reexamined and subjected to a more rigorous individual inspection of vacuolar morphology (see *Materials and Methods*). Of these 77 strains, those that yielded cells containing mostly one or two vacuoles after treatment with Tm were considered the strongest candidates for further study (Figure 7B and Supplemental Table S2).

As expected, genes identified in our screen included factors determined previously to be required for fragmentation in response to hyperosmotic stress, including PI(3,5)P_2 biosynthesis (Fab1, Vps15), components of the vacuolar ATPase (Vma3, Vma6), and members of the AP-3 adaptor complex (Aps3, Apl5, Apm3), as well as components involved in TORC1 signaling (Sit4, Vps9; Bonangelino *et al.*, 2002; Baars *et al.*, 2007; Bridges *et al.*, 2012; Michaillat and Mayer, 2013; Figure 7B and Supplemental Table S1). In addition, our screen identified several new genes involved in vacuolar fragmentation that belong to virtually all functional groups (e.g., APL6, HIM1, and VPS15; Figure 7B and Supplemental Table S2). Of interest, one new functional group consisted of genes, including VPH2 and VMA21, that are involved in V-ATPase assembly (Figure 7B). Finally, our strongest hits included a number of genes that are unique to ER

stress–induced fragmentation and encode proteins localized to the ER and Golgi (ATG8, EPS1, ALG9, GVP36), suggesting a potentially important role for the secretory pathway for this response (Supplemental Table S1).

Evidence that Vph2 provides a linkage between TORC1 and vacuolar fission

To begin to explore the role of newly identified components in vacuolar fission, we assessed the intracellular localization of representative GFP-tagged proteins from each category of our strongest candidates (Figure 7B), both in the absence and after treatment with Tm. Before drug treatment, all nine proteins displayed distinct localization patterns throughout the cell, consistent with previously published observations (Figure 8A). For all but one of these candidates, no change in distribution was observed after Tm treatment, indicating their localization was not influenced by ER stress (Figure 8A). The sole exception was Vph2, which was localized in a uniform manner throughout the ER in the absence of Tm but adopted a discontinuous punctate pattern within the ER after drug treatment (Figure 8, A and B). Because of the link we established between TORC1 signaling and vacuolar fragmentation, we asked whether this Tm-induced change in Vph2 localization was dependent on TORC1 activity. To test this, we examined Vph2 after simultaneous treatment of cells with both Tm and rapamycin and observed that rapamycin blocked completely the transition of Vph2 into a punctate localization pattern (Figure 8B). Tm treatment did not affect the overall stability of the Vph2-GFP fusion protein used for this experiment, demonstrating that the punctate localization pattern was not due, for example, to the generation of free GFP (Supplemental Figure S6). We conclude from these findings that TORC1 activity is required for ER stress–catalyzed changes in Vph2 localization.

Loss of Vph2 results in the Vma^- phenotype characteristic of V-ATPase mutants and includes defects in acidification of the vacuole (Preston *et al.*, 1989; Bachhawat *et al.*, 1993; Hirata *et al.*, 1993; Jackson and Stevens, 1997; Graham and Stevens, 1999). Indeed, Vph2 has been suggested to stabilize components of the V-ATPase and therefore aid in its assembly (Hirata *et al.*, 1993; Graham *et al.*, 1998). Evidence exists that vacuolar acidification is required for fission (Baars *et al.*, 2007; Kim *et al.*, 2012); however, the precise role of the V-ATPase in vacuolar morphology has been somewhat controversial, with proposed roles in fusion that are distinct from a requirement for acidification alone (Bayer *et al.*, 2003; Takeda *et al.*, 2008). We therefore sought to determine the relationship between Vph2 and vacuolar pH with respect to ER stress–induced vacuolar fragmentation. First, we confirmed that a *vph2Δ* mutant possessed a strong acidification defect, based on its failure to grow at neutral pH, similar to the V-ATPase mutant *vma7Δ* (Figure 9A). Growth of both strains was rescued by buffering the culture medium to pH 5.5, which correlated with WT levels of vacuolar acidification, as assayed using the fluorescent pH-reactive indicator dye 5(6)–carboxyfluorescein diacetate (CFDA; Figure 9A, inset). Remarkably, despite this rescue in vacuolar acidification, however, we observed that both *vph2Δ* and *vma7Δ* cells remained blocked in vacuolar fission after treatment with Tm (Figure 9B). These findings suggest that the function of Vph2, as well as of the V-ATPase in general, may include roles distinct from acidification to regulate ER stress–induced fragmentation.

DISCUSSION

We combined genomic, biochemical, and cell biological approaches to explore the link between perturbation of ER homeostasis, induced by the protein misfolding agents Tm and DTT, and the process of vacuolar fragmentation. We determined that this link involves components and activities required for normal vacuolar function and morphology, including synthesis of $PI(3,5)P_2$, the V-ATPase, the AP-3 clathrin-associated adaptor complex, and the class C core vacuole/endosome membrane tethering complex. Because many of these components have been shown to be required for vacuolar fission, we argue that ER stress is likely to interface with the vacuolar fission machinery to stimulate fragmentation. Remarkably, we determined that none of the canonical signaling pathways that respond to ER stress, including the UPR, ERAD, and ERSU pathways, is required for ER stress–induced vacuolar fragmentation, suggesting that a previously uncharacterized signaling pathway is involved in this process. In this regard, our demonstration of a requirement for TORC1, as well as two of its downstream effector arms, defined by Sch9 and Tap42/Sit4, respectively, is significant and indicates that TORC1 signaling plays an integral role in vacuolar morphology, for which we propose that TORC1 is likely to function in parallel with ER stress to regulate vacuolar fragmentation.

Our proposed role for TORC1 in ER stress–induced vacuolar fragmentation is consistent with previous findings that this complex is required for changes in vacuolar morphology in response to hyperosmotic stress (Michaillat *et al.*, 2012). In particular, a system for recapitulating salt-sensitive vacuolar fragmentation in vitro demonstrated this process is sensitive to rapamycin, as well as to loss of the nonessential TORC1 subunit Tco89 (Michaillat *et al.*, 2012). These authors found further that hyperosmotic shock–induced fragmentation was impaired in *sit4Δ* cells, consistent with our results that TORC1 functions through this phosphatase to influence vacuolar morphology. In contrast to our present findings, however, these authors did not observe a role for either Tap42 or Sch9, indicating there are likely to be important differences in the signaling requirements that link these two stress responses to changes in vacuolar morphology. We note that the kinetics of the two responses are also significantly different; salt-induced fragmentation occurs on a time scale of minutes, whereas ER stress requires ~2 h for maximum fragmentation to occur. Moreover, a comparison of results of our genome-wide screen for mutants defective in ER stress–induced fragmentation and a similar screen that identified mutants defective in salt-induced fragmentation (Michaillat and Mayer, 2013) reveals that there is an overlapping yet nonidentical set of components involved in these processes (Supplemental Table S2). Nevertheless, because there is significant overlap in genes identified in the two screens, it is likely that both ER stress and hyperosmotic stress converge on a core set of components required for vacuolar fission.

One of these components is Fab1, the PI 3-phosphate 5-kinase responsible for synthesis of $PI(3,5)P_2$, a lipid that is enriched at the outer vacuolar membrane and is required for fission, the levels of which, moreover, increase after hyperosmotic stress (Dove *et al.*, 1997; Cooke *et al.*, 1998; Bonangelino *et al.*, 2002). Of interest, a link between $PI(3,5)P_2$ and TORC1 was reported in which an inverse correlation was observed between levels of this lipid and the sensitivity of cells to rapamycin (Bridges *et al.*, 2012). In addition, the TORC1-specific component Kog1, orthologue of the mammalian mTORC1 subunit Raptor, binds to $PI(3,5)P_2$ at the vacuolar membrane (Bridges *et al.*, 2012). Thus it is possible that $PI(3,5)P_2$ recruits TORC1 and/or its effectors to sites of vacuolar fission and thereby regulates the activity of substrates involved in fission. Alternatively, $PI(3,5)P_2$ and TORC1 may alter the lipid environment of the vacuolar membrane to stimulate fission, where it has been reported that formation of lipid microdomains within the vacuolar membrane required both Fab1 and the activity of TORC1 (Toulmay and Prinz, 2013). The substrate for Fab1 is PI 3-phosphate, which is produced

A

	Localization	
ORF	-Tm	+Tm
Vps9	Cytosol	No Change
Vma6	Vacuole/Vacuole Membrane	No Change
Vma7	Vacuole/Vacuole Membrane	No Change
Vph2	ER	Punctate
Vma21	Vacuole/Vacuole Membrane	No Change
Apl6	Punctate/Golgi	No Change
Vps3	Punctate	No Change
Vps15	Punctate/Vacuole	No Change
Cys4	Cytosol	No Change

B

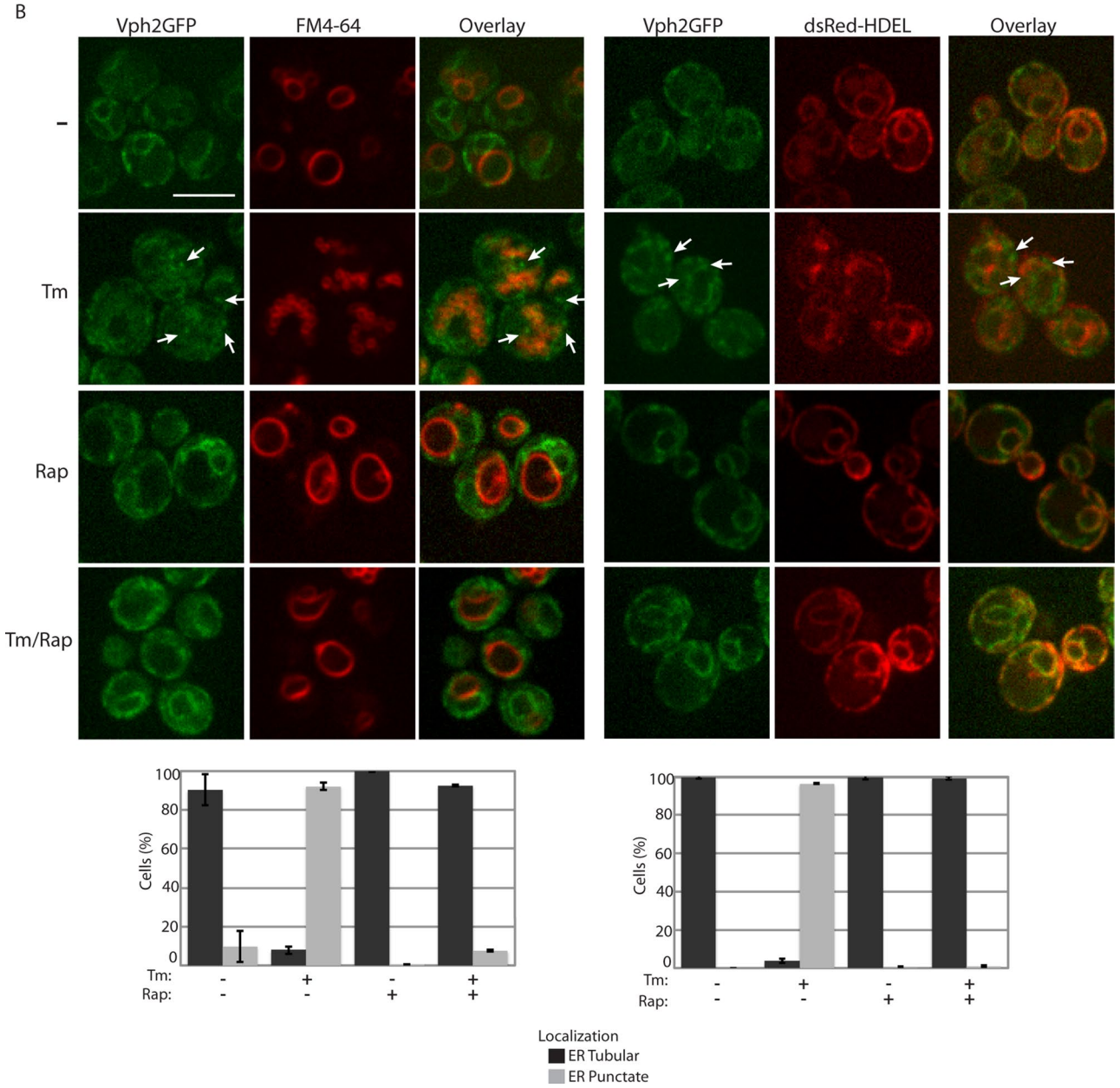

FIGURE 8: ER stress elicits changes in Vph2GFP distribution. (A) Table indicating GFP localization of C-terminally tagged proteins from the yeast GFP collection. Strains were grown, treated with DMSO (DM) and Tm as described in Figure 1, and imaged as described in Figure 4. (B) Vph2GFP (BY4741) was grown overnight at 30°C to early log phase (OD_{600} = 0.25) in YPD + 1 μM FM4-64 medium, treated with DMSO, 1 μg/ml Tm, 200 nM Rap, or both 1 μg/ml Tm and 200 nM Rap for 2 h, and then centrifuged and immediately visualized using fluorescence microscopy. Vph2GFP cells containing dsRED-HDEL (PLY1641) were grown to early log phase, treated with DMSO, 1 μg/ml Tm, 200 nM Rap, or both 1 μg/ml Tm and 200 nM Rap for 2 h, and imaged as described in Figure 4. Scale bar, 5 μm. GFP signal was scored as either ER localized (ER Tubular) or as punctate within the ER (ER Punctate). Averages of three independent experiments are presented ± SEM. Arrowheads show Vph2 puncta.

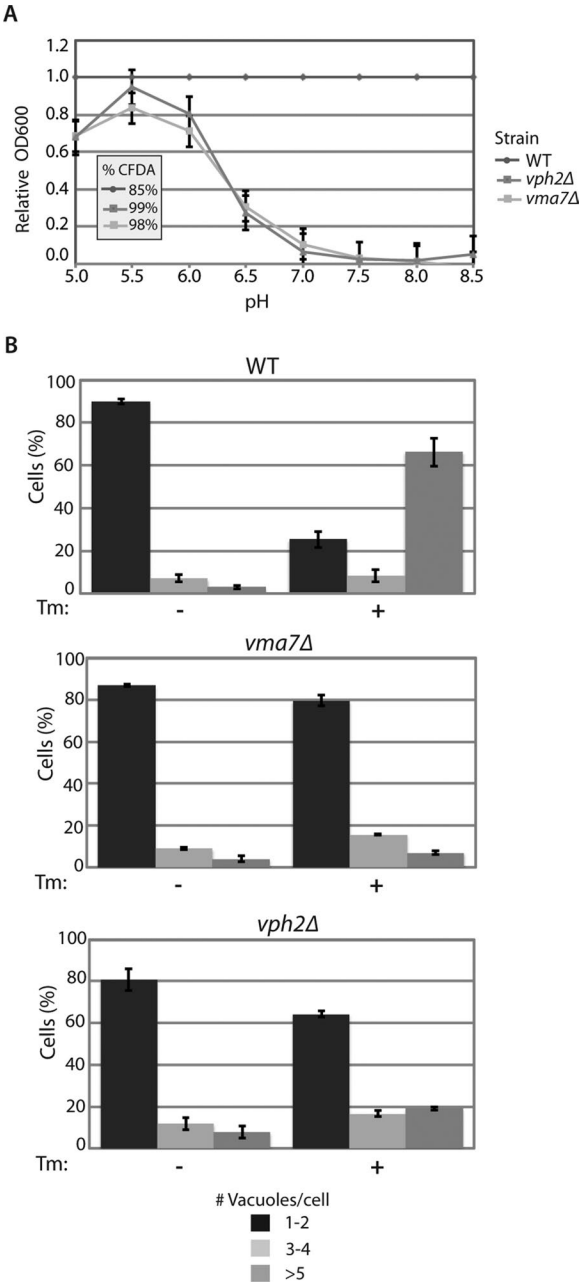

FIGURE 9: Vacuolar acidification does not restore *vph2Δ* vacuolar fragmentation defects. (A) WT (BY4741), *vph2Δ*, and *vma7Δ* cells were grown in YPD medium buffered to the indicated pH level with MES. Medium was inoculated at OD_{600} = 0.025 and grown overnight at 30°C for 16 h. Average measurement of the OD_{600} compared with WT in three independent experiments is presented ± SEM. Inset, percentage of cells with vacuolar CFDA staining after incubation in pH 5.5 YPD medium as described in D. (B) WT (BY4741), *vph2Δ*, and *vma7Δ* cells were grown overnight at 30°C to early log phase, and then 5 μM FM4-64 was added to the YPD medium and cells were incubated 1 h at 30°C. Cells were resuspended in fresh YPD, pH 5.5, medium containing DMSO or Tm (1 μg/ml) and incubated for 2 h at 30°C. CFDA, 10 μM, was added to the medium during the last 30 min. Cells were centrifuged, and vacuolar morphology and CFDA staining was assessed using fluorescence microscopy.

by Vps34, the sole PI 3-kinase in yeast (Auger *et al.*, 1989). Although this enzyme was not identified in our genomic screen, we subsequently examined *vps34Δ* cells and determined that there is a significant (~30%) defect in ER stress–induced vacuolar fragmentation (unpublished observations). In addition, we observed a range of additional mild vacuolar morphology defects in *vps34Δ* cells both in the presence and absence of treatment with Tm, consistent with prior characterization of *vps34* as a class D *vps* mutant (Raymond *et al.*, 1992). We do not understand why *vps34Δ* cells possess a more mild fragmentation defect than *fab1Δ* cells, but this may be related to fact that PI 3-phosphate both is the precursor to the synthesis of $PI(3,5)P_2$ and is involved directly in vacuolar fusion (Boeddinghaus *et al.*, 2002).

Our genome-wide screen also revealed a role for structural components of the V-ATPase, as well as two additional factors required for V-ATPase assembly, Vph2 and Vma21, in ER stress–induced vacuolar fragmentation. Previous studies demonstrated that the V-ATPase is required for vacuolar fragmentation during hyperosmotic stress, as well as for vacuolar fusion (Bayer *et al.*, 2003; Baars *et al.*, 2007; Takeda *et al.*, 2008; Kim *et al.*, 2012). What remains controversial, however, is whether the V-ATPase simply provides an acidified internal environment important for fission and/or fusion or might play a more fundamental mechanistic role in these processes (Ungermann *et al.*, 1999; Bayer *et al.*, 2003; Coonrod *et al.*, 2013). In this context, it is significant that although we were able to correct the vacuolar acidification defects associated with both Vph2 and Vma7, a component of the V1 domain of the V-ATPase, this was insufficient to restore ER stress–induced fragmentation within these cells. One possibility is that vacuolar acidification is necessary but not sufficient for fragmentation in response to ER stress and that the V-ATPase plays an additional role(s) important for changes in vacuolar morphology. Of importance, Tm treatment does not affect the distribution of V-ATPase subunits Vma6 and Vma7 at the vacuole (Figure 8A), consistent with a requirement for the V-ATPase to be present at the vacuole during fragmentation.

In mammalian cells, the V-ATPase has been identified as a regulator of mTORC1 activation in response to amino acid availability (Zoncu *et al.*, 2011). In particular, interactions between the V-ATPase and the p14 subunit of the Ragulator complex are proposed to modulate mTORC1 activity in response to amino acids (Zoncu *et al.*, 2011). In this regard, it is relevant that our genomic screen identified Ego3 as being important for ER stress–induced vacuolar fragmentation (Supplemental Table S1 and Supplemental Figure S5). This protein is a subunit of the EGO complex and, like Ragulator, regulates TORC1 activity at the vacuolar membrane (Binda *et al.*, 2009). Moreover, Ego3 forms a homodimer in a manner similar to the p14-MP1 heterodimer, and these components have been proposed to be functional homologues (Zhang *et al.*, 2012). Thus it is possible that the EGO complex, in particular the Ego3 subunit, is required for TORC1 activity in response to ER stress. However, as described earlier (Supplemental Figure S5), the behavior of other EGO complex mutants does not support such a role, suggesting that the activity of this complex in regulating TORC1 during vacuolar fragmentation would necessarily be complex.

Finally, our findings highlight the emerging importance of functional interactions between organelles and their roles in diverse cell biological processes. In many cases, these interactions are mediated by direct physical contact between membranes at distinct regions termed membrane contact sites (Helle *et al.*, 2013). In particular, the vacuole is known to contact both the ER and the nuclear membrane at nucleus–vacuole junctions, which are important for piecemeal microautophagy at the nucleus, a process mediated by TORC1 (Roberts *et al.*, 2003). More recently, a novel contact site between the ER and the vacuole has been described that is required for formation of specific membrane domains that form in response

Strain	Genotype	Source
W303α	*MATα ade2-1; leu2-3112; his3-11, 15; trp1-1; ura3-1; can1-100*	Naysmyth *et al.* (1990)
PLY1637	W303α, except *ire1*::HIS3	This study
PLY553	W303α, except *tap42*::HIS3 + [pRS414 (CEN4 TRP1)-TAP42]	Duvel *et al.* (2003)
PLY551	W303α, except *tap42*::HIS3 + [pRS414 (CEN4 TRP1)-*tap42-106*]	Duvel *et al.* (2003)
PLY1638	W303α, except *sit4*::KANMX6	This study
PLY1639	W303α, except sch9::HIS3	This study
PLY1640	W303α, TCO89-yEGFP-Kan	This study
BY4741	his3*Δ*1; leu2*Δ*0; met15*Δ*0; ura3*Δ*0	Brachmann *et al.* (1998)
TB50a	*MATa* leu2-3112 ura3-52 rme1 trp1 his3	Sturgill *et al.* (2008)
PLY1176	*MATa* leu2-3112 ura3-52 rme1 trp1 his3 TOR1D330-3XGFP HMLa/pSH47 [CEN URA3]	Sturgill *et al.* (2008)
PLY1641	*MATa* his3*Δ*1 leu2*Δ*0 met15*Δ*0 ura3*Δ*0, Vph2GFP-His3MX6, *dsRed*-HDEL	This study
PLY1642	*MATα, leu2-3112,trp1-1, can1-100, ura3-1, ade2-1, his3-11, bar1Δ::LEU2*	Babour *et al.* (2010)
PLY1643	*MATα, leu2-3112,trp1-1, can1-100, ura3-1, ade2-1, his3-11,15, ero1-1*::HIS3, *bar1Δ*::LEU2	Babour *et al.* (2010)

TABLE 1: *Saccharomyces cerevisiae* strains used in this study.

to stress and include the TORC1-specific component Kog1 (Murley *et al.*, 2015). Thus it is tempting to speculate that TORC1 may localize to ER–vacuole contact sites and that this may play a role in its regulation of changes in vacuolar morphology, including vacuolar fragmentation in response to ER stress.

MATERIALS AND METHODS

Yeast strains, plasmids, and media

Yeast strains used in this study are listed in Table 1. Strains from the yeast haploid deletion collection (Giaever *et al.*, 2002) and the yeast GFP library (Huh *et al.*, 2003) were used in indicated figure legends. Cells were grown in either rich YPD (2% yeast extract, 1% peptone, and 2% dextrose) or synthetic complete dextrose medium (0.8% yeast nitrogen base without amino acids, pH 5.5, 2% dextrose) supplemented with amino acids as described previously (Sherman, 1991). The Npr1HA and Par32HA plasmids described by Graef and Nunnari (2011) and Huber *et al.* (2009), respectively, were transformed into W303α cells using a previously described lithium acetate procedure (Gietz and Woods, 2002). Deletion strains were constructed by knockout of the complete open reading frame with a selectable marker as previously described (Dilova *et al.*, 2002). TCO89 was endogenously tagged with GFP using the pKT127 (pFA6a–link–yEGFP–Kan) cassette described by Sheff and Thorn (2004). To create PLY1641, TIPlac-dsRED-HDEL as described in Madrid *et al.* (2006) was linearized with *Eco*RV for integration and transformed into Vph2GFP (BY4741) from the GFP library (Huh *et al.*, 2003).

Tunicamycin was dissolved in dimethyl sulfoxide (DMSO) and added to culture medium at a final concentration of 1 μg/ml. DTT (25 μM), rapamycin (200 nM), and cycloheximide (25 mg/ml) were dissolved in DMSO and added to culture medias as described in the respective figure legends. 5(6)-CFDA was added to culture medium to a final concentration of 10 μM after resuspension of cells in YPD, pH 5.5, medium buffered with 2-(*N*-morpholino)ethanesulfonic (MES) acid as described previously (Vida and Emr, 1995).

Vacuolar fragmentation assay

Vacuolar membrane labeling was done by growing cells overnight at 30°C to logarithmic phase ($OD_{600} < 1$) in YPD or selective medium containing 1 μM FM4-64. Cells were adjusted to $OD_{600} = 0.25$ and then treated with drugs as described and incubated at 30°C for 2 h. Cells were pelleted by centrifugation, resuspended in residual medium, and imaged using fluorescence microscopy as described later. Vacuolar morphology was quantified by counting the number of vacuoles per cell (100 cells/condition), then grouped into three categories: cells containing 1–2, 3–4, or ≥5 vacuoles per cell, as described previously (Michaillat *et al.*, 2012). Averages of three independent experiments are presented with ± SEM.

Whole-cell extraction, Western blot analysis, and quantification

Protein extracts were prepared using a NaOH cell lysis method (Dilova *et al.*, 2002), loaded onto SDS–PAGE gels, and transferred to nitrocellulose membrane. Membranes were probed with anti-hemagglutinin (HA; 1:5000; Sigma-Aldrich, St. Louis, MO), anti–glucose-6-phosphate dehydrogenase (G6PDH; Zwf1; 1:100,000; Sigma-Aldrich), or anti-GFP (1 μg/ml; N86/8; Neuromab, Davis, CA) primary antibodies and visualized using the appropriate secondary antibodies conjugated to IR Dye (1:5000; Li-COR Biosciences, Lincoln, NE). Quantifications were performed using ImageQuant software (GE Healthcare, Little Chalfont, UK). The relative distribution of the signal in each lane was figured by measuring the level of signal in three distinct portions of each lane—upper (hyperphosphorylated), center (phosphorylated), and lower (dephosphorylated)—and then dividing each portion by the total amount of signal within each lane.

Fluorescence microscopy

Strains containing fluorescently tagged proteins were labeled with FM4-64 as described and examined using the spinning-disk module of a Marianas SDC Real Time 3D Confocal-TIRF microscope (Intelligent Imaging Innovations, Denver, CO) fitted with a Yokogawa spinning-disk head, a 100×/1.46 numerical aperture objective, and an electron-multiplying charge-coupled device (EMCCD) camera. *Z*-stacks were taken at 0.4-μm increments over ~6 μm of the cell. Images were processed using ImageJ software (National Institutes of Health, Bethesda, MD). Colocalization of GFP signal to FM4-64 was quantified using Imaris software (Bitplane, Concord, MA). The Manders coefficients are displayed. Assessment of vacuolar morphology and 5(6)-CFDA staining in strains without GFP-tagged proteins was

performed using a Nikon E600 fluorescence microscope and an Orca ER CCD camera (Hamamatsu, Hamamatsu, Japan) controlled by Micro Manager 1.2 ImageJ software.

Genome-wide screen

Strains from the haploid deletion collection (Giaever *et al.*, 2002) were grown in 384-well plates overnight in YPD medium plus 1 μM FM4-64 at 30°C, then diluted 1:25 with fresh medium for 3 h to allow for logarithmic growth. YPD containing 1 μg/ml Tm was added to each well, and cells were incubated at 30°C for 90 min and then transferred to concanavalin A (0.25 mg/ml)–treated 384-well, glass-bottomed microscopy plates (Greiner Bio-One, Frickenhausen, Germany) for 15 min at ambient temperature. Cells were washed three times with YPD and imaged using the CellVoyager CV1000 confocal system, a 60× water immersion objective, and the back-illuminated EMCCD camera supplied with the unit (Yokogawa, Tokyo, Japan). Deletion strains with 50% or more of cells displaying a defect in vacuolar fragmentation (nonfragmented vacuoles) after the initial pass were rearrayed using a RoToR robot (Singer Instruments, Somerset, UK) to form a new library of candidate hits. This library was assayed twice more as described, after treatment with YPD containing DMSO, 1 μg/ml Tm, or 25 μM DTT. The defect in vacuolar fragmentation of each hit was judged by estimating the percentage of cells with nonfragmented vacuoles after Tm treatment, and then strains were grouped into one of three categories: cells containing 50–70, 70–90, or 90–100% nonfragmented vacuoles. Hits with >50% of nonfragmented vacuoles (315) were manually grouped into 12 functional categories according to their involvement in cellular processes identified using the Saccharomyces Genome Database (Figure 6A).

From the 315 identified hits, deletion strains with the strongest fragmentation defects (70–100% nonfragmented vacuoles) and 14 hits involved in cellular signaling were rearrayed to form a top-hits library containing 77 strains. Vacuolar morphology in this top-hits library was examined following DMSO, Tm, and DTT treatment as described, except that vacuolar structure was visualized using a Nikon Eclipse Ti with a 60× oil immersion 1.4 NA objective and Zyla sCMOS camera (Andor, Belfast, Northern Ireland) run by the Nikon high-content analysis package running inside Nikon Elements. The fragmentation defect in these strains was thoroughly quantified as described.

ACKNOWLEDGMENTS

We thank Martin Graef and Robbie Loewith for providing Npr1HA and Par32HA plasmids and members of T.P.'s laboratory, Jodi Nunnari, and members of the Nunnari laboratory for critical discussions and comments. We thank Eric Tieu, Amelia Joslin, Renan Lopes, and Nerea Muniozguren for technical help and meaningful discussions in completing this study. This work was supported by National Institutes of Health Grant GM086387 (to T.P.).

REFERENCES

Auger KR, Carpenter CL, Cantley LC, Varticovski L (1989). Phosphatidylinositol 3-kinase and its novel product, phosphatidylinositol 3-phosphate, are present in Saccharomyces cerevisiae. J Biol Chem 264, 20181–20184.

Baars TL, Petri S, Peters C, Mayer A (2007). Role of the V-ATPase in regulation of the vacuolar fission-fusion equilibrium. Mol Biol Cell 18, 3873–3882.

Baba M, Takeshige K, Baba N, Ohsumi Y (1994). Ultrastructural analysis of the autophagic process in yeast: detection of autophagosomes and their characterization. J Cell Biol 124, 903–913.

Babour A, Bicknell AA, Tourtellotte J, Niwa M (2010). A surveillance pathway monitors the fitness of the endoplasmic reticulum to control its inheritance. Cell 142, 256–269.

Bachhawat AK, Manolson MF, Murdock DG, Garman JD, Jones EW (1993). The VPH2 gene encodes a 25 kDa protein required for activity of the yeast vacuolar H(+)-ATPase. Yeast 9, 175–184.

Banta LM, Robinson JS, Klionsky DJ, Emr SD (1988). Organelle assembly in yeast: characterization of yeast mutants defective in vacuolar biogenesis and protein sorting. J Cell Biol 107, 1369–1383.

Bayer MJ, Reese C, Buhler S, Peters C, Mayer A (2003). Vacuole membrane fusion: V0 functions after trans-SNARE pairing and is coupled to the Ca2+-releasing channel. J Cell Biol 162, 211–222.

Bays NW, Gardner RG, Seelig LP, Joazeiro CA, Hampton RY (2001). Hrd1p/Der3p is a membrane-anchored ubiquitin ligase required for ER-associated degradation. Nat Cell Biol 3, 24–29.

Beugnet A, Tee AR, Taylor PM, Proud CG (2003). Regulation of targets of mTOR (mammalian target of rapamycin) signalling by intracellular amino acid availability. Biochem J 372, 555–566.

Bicknell AA, Tourtellotte J, Niwa M (2010). Late phase of the endoplasmic reticulum stress response pathway is regulated by Hog1 MAP kinase. J Biol Chem 285, 17545–17555.

Binda M, Peli-Gulli MP, Bonfils G, Panchaud N, Urban J, Sturgill TW, Loewith R, De Virgilio C (2009). The Vam6 GEF controls TORC1 by activating the EGO complex. Mol Cell 35, 563–573.

Boeddinghaus C, Merz AJ, Laage R, Ungermann C (2002). A cycle of Vam7p release from and PtdIns 3-P-dependent rebinding to the yeast vacuole is required for homotypic vacuole fusion. J Cell Biol 157, 79–89.

Bonangelino CJ, Nau JJ, Duex JE, Brinkman M, Wurmser AE, Gary JD, Emr SD, Weisman LS (2002). Osmotic stress-induced increase of phosphatidylinositol 3,5-bisphosphate requires Vac14p, an activator of the lipid kinase Fab1p. J Cell Biol 156, 1015–1028.

Bonilla M, Nastase KK, Cunningham KW (2002). Essential role of calcineurin in response to endoplasmic reticulum stress. EMBO J 21, 2343–2353.

Brachmann CB, Davies A, Cost GJ, Caputo E, Li J, Hieter P, Boeke JD (1998). Designer deletion strains derived from Saccharomyces cerevisiae S288C: a useful set of strains and plasmids for PCR-mediated gene disruption and other applications. Yeast 14, 115–132.

Bridges D, Fisher K, Zolov SN, Xiong T, Inoki K, Weisman LS, Saltiel AR (2012). Rab5 proteins regulate activation and localization of target of rapamycin complex 1. J Biol Chem 287, 20913–20921.

Bridges D, Ma JT, Park S, Inoki K, Weisman LS, Saltiel AR (2012). Phosphatidylinositol 3,5-bisphosphate plays a role in the activation and subcellular localization of mechanistic target of rapamycin 1. Mol Biol Cell 23, 2955–2962.

Cardenas ME, Heitman J (1995). FKBP12-rapamycin target TOR2 is a vacuolar protein with an associated phosphatidylinositol-4 kinase activity. EMBO J 14, 5892–5907.

Cooke FT, Dove SK, McEwen RK, Painter G, Holmes AB, Hall MN, Michell RH, Parker PJ (1998). The stress-activated phosphatidylinositol 3-phosphate 5-kinase Fab1p is essential for vacuole function in S. cerevisiae. Curr Biol 8, 1219–1222.

Coonrod EM, Graham LA, Carpp LN, Carr TM, Stirrat L, Bowers K, Bryant NJ, Stevens TH (2013). Homotypic vacuole fusion in yeast requires organelle acidification and not the V-ATPase membrane domain. Dev Cell 27, 462–468.

Cox JS, Shamu CE, Walter P (1993). Transcriptional induction of genes encoding endoplasmic reticulum resident proteins requires a transmembrane protein kinase. Cell 73, 1197–1206.

Deak PM, Wolf DH (2001). Membrane topology and function of Der3/Hrd1p as a ubiquitin-protein ligase (E3) involved in endoplasmic reticulum degradation. J Biol Chem 276, 10663–10669.

Di Como CJ, Arndt KT (1996). Nutrients, via the Tor proteins, stimulate the association of Tap42 with type 2A phosphatases. Genes Dev 10, 1904–1916.

Dilova I, Chen CY, Powers T (2002). Mks1 in concert with TOR signaling negatively regulates RTG target gene expression in S. cerevisiae. Curr Biol 12, 389–395.

Dove SK, Cooke FT, Douglas MR, Sayers LG, Parker PJ, Michell RH (1997). Osmotic stress activates phosphatidylinositol-3,5-bisphosphate synthesis. Nature 390, 187–192.

Dove SK, McEwen RK, Mayes A, Hughes DC, Beggs JD, Michell RH (2002). Vac14 controls PtdIns(3,5)P(2) synthesis and Fab1-dependent protein trafficking to the multivesicular body. Curr Biol 12, 885–893.

Dubouloz F, Deloche O, Wanke V, Cameroni E, De Virgilio C (2005). The TOR and EGO protein complexes orchestrate microautophagy in yeast. Mol Cell 19, 15–26.

Duvel K, Santhanam A, Garrett S, Schneper L, Broach JR (2003). Multiple roles of Tap42 in mediating rapamycin-induced transcriptional changes in yeast. Mol Cell 11, 1467–1478.

Frand AR, Kaiser CA (1998). The ERO1 gene of yeast is required for oxidation of protein dithiols in the endoplasmic reticulum. Mol Cell 1, 161–170.
Gander S, Bonenfant D, Altermatt P, Martin DE, Hauri S, Moes S, Hall MN, Jenoe P (2008). Identification of the rapamycin-sensitive phosphorylation sites within the Ser/Thr-rich domain of the yeast Npr1 protein kinase. Rapid Commun Mass Spectrom 22, 3743–3753.
Gao M, Kaiser CA (2006). A conserved GTPase-containing complex is required for intracellular sorting of the general amino-acid permease in yeast. Nat Cell Biol 8, 657–667.
Giaever G, Chu AM, Ni L, Connelly C, Riles L, Veronneau S, Dow S, Lucau-Danila A, Anderson K, Andre B, *et al.* (2002). Functional profiling of the Saccharomyces cerevisiae genome. Nature 418, 387–391.
Gietz RD, Woods RA (2002). Transformation of yeast by lithium acetate/single-stranded carrier DNA/polyethylene glycol method. Methods Enzymol 350, 87–96.
Graef M, Nunnari J (2011). Mitochondria regulate autophagy by conserved signalling pathways. EMBO J 30, 2101–2114.
Graham LA, Hill KJ, Stevens TH (1998). Assembly of the yeast vacuolar H+-ATPase occurs in the endoplasmic reticulum and requires a Vma12p/Vma22p assembly complex. J Cell Biol 142, 39–49.
Graham LA, Stevens TH (1999). Assembly of the yeast vacuolar proton-translocating ATPase. J Bioenerg Biomembr 31, 39–47.
Helle SC, Kanfer G, Kolar K, Lang A, Michel AH, Kornmann B (2013). Organization and function of membrane contact sites. Biochim Biophys Acta 1833, 2526–2541.
Hirata R, Umemoto N, Ho MN, Ohya Y, Stevens TH, Anraku Y (1993). VMA12 is essential for assembly of the vacuolar H(+)-ATPase subunits onto the vacuolar membrane in Saccharomyces cerevisiae. J Biol Chem 268, 961–967.
Huber A, Bodenmiller B, Uotila A, Stahl M, Wanka S, Gerrits B, Aebersold R, Loewith R (2009). Characterization of the rapamycin-sensitive phosphoproteome reveals that Sch9 is a central coordinator of protein synthesis. Genes Dev 23, 1929–1943.
Huh WK, Falvo JV, Gerke LC, Carroll AS, Howson RW, Weissman JS, O'Shea EK (2003). Global analysis of protein localization in budding yeast. Nature 425, 686–691.
Jackson DD, Stevens TH (1997). VMA12 encodes a yeast endoplasmic reticulum protein required for vacuolar H+-ATPase assembly. J Biol Chem 272, 25928–25934.
Jamsa E, Simonen M, Makarow M (1994). Selective retention of secretory proteins in the yeast endoplasmic reticulum by treatment of cells with a reducing agent. Yeast 10, 355–370.
Jiang Y, Broach JR (1999). Tor proteins and protein phosphatase 2A reciprocally regulate Tap42 in controlling cell growth in yeast. EMBO J 18, 2782–2792.
Kamada Y, Yoshino K, Kondo C, Kawamata T, Oshiro N, Yonezawa K, Ohsumi Y (2010). Tor directly controls the Atg1 kinase complex to regulate autophagy. Mol Cell Biol 30, 1049–1058.
Kim E, Goraksha-Hicks P, Li L, Neufeld TP, Guan KL (2008). Regulation of TORC1 by Rag GTPases in nutrient response. Nat Cell Biol 10, 935–945.
Kim H, Kim A, Cunningham KW (2012). Vacuolar H+-ATPase (V-ATPase) promotes vacuolar membrane permeabilization and nonapoptotic death in stressed yeast. J Biol Chem 287, 19029–19039.
Lempiainen H, Uotila A, Urban J, Dohnal I, Ammerer G, Loewith R, Shore D (2009). Sfp1 interaction with TORC1 and Mrs6 reveals feedback regulation on TOR signaling. Mol Cell 33, 704–716.
Li SC, Kane PM (2009). The yeast lysosome-like vacuole: endpoint and crossroads. Biochim Biophys Acta 1793, 650–663.
Loewith R, Hall MN (2011). Target of rapamycin (TOR) in nutrient signaling and growth control. Genetics 189, 1177–1201.
Madrid AS, Mancuso J, Cande WZ, Weis K (2006). The role of the integral membrane nucleoporins Ndc1p and Pom152p in nuclear pore complex assembly and function. J Cell Biol 173, 361–371.
McCracken AA, Karpichev IV, Ernaga JE, Werner ED, Dillin AG, Courchesne WE (1996). Yeast mutants deficient in ER-associated degradation of the Z variant of alpha-1-protease inhibitor. Genetics 144, 1355–1362.
Michaillat L, Baars TL, Mayer A (2012). Cell-free reconstitution of vacuole membrane fragmentation reveals regulation of vacuole size and number by TORC1. Mol Biol Cell 23, 881–895.
Michaillat L, Mayer A (2013). Identification of genes affecting vacuole membrane fragmentation in Saccharomyces cerevisiae. PLoS One 8, e54160.
Murley A, Sarsam RD, Toulmay A, Yamada J, Prinz WA, Nunnari J (2015). Ltc1 is an ER-localized sterol transporter and a component of ER-mitochondria and ER-vacuole contacts. J Cell Biol 209, 539548.
Nasmyth K, Adolf G, Lydall D, Seddon A (1990). The identification of a second cell cycle control on the HO promoter in yeast: cell cycle regulation of SW15 nuclear entry. Cell 62, 631–647.
Okamura K, Kimata Y, Higashio H, Tsuru A, Kohno K (2000). Dissociation of Kar2p/BiP from an ER sensory molecule, Ire1p, triggers the unfolded protein response in yeast. Biochem Biophys Res Commun 279, 445–450.
Powis K, Zhang T, Panchaud N, Wang R, Virgilio CD, Ding J (2015). Crystal structure of the Ego1-Ego2-Ego3 complex and its role in promoting Rag GTPase-dependent TORC1 signaling. Cell Res 25, 1043–1059.
Preston RA, Murphy RF, Jones EW (1989). Assay of vacuolar pH in yeast and identification of acidification-defective mutants. Proc Natl Acad Sci USA 86, 7027–7031.
Raymond CK, Howald-Stevenson I, Vater CA, Stevens TH (1992). Morphological classification of the yeast vacuolar protein sorting mutants: evidence for a prevacuolar compartment in class E vps mutants. Mol Biol Cell 3, 1389–1402.
Roberts P, Moshitch-Moshkovitz S, Kvam E, O'Toole E, Winey M, Goldfarb DS (2003). Piecemeal microautophagy of nucleus in Saccharomyces cerevisiae. Mol Biol Cell 14, 129–141.
Rutkowski DT, Kaufman RJ (2004). A trip to the ER: coping with stress. Trends Cell Biol 14, 20–28.
Sancak Y, Peterson TR, Shaul YD, Lindquist RA, Thoreen CC, Bar-Peled L, Sabatini DM (2008). The Rag GTPases bind raptor and mediate amino acid signaling to mTORC1. Science 320, 1496–1501.
Schmidt A, Beck T, Koller A, Kunz J, Hall MN (1998). The TOR nutrient signalling pathway phosphorylates NPR1 and inhibits turnover of the tryptophan permease. EMBO J 17, 6924–6931.
Schuck S, Prinz WA, Thorn KS, Voss C, Walter P (2009). Membrane expansion alleviates endoplasmic reticulum stress independently of the unfolded protein response. J Cell Biol 187, 525–536.
Sheff MA, Thorn KS (2004). Optimized cassettes for fluorescent protein tagging in Saccharomyces cerevisiae. Yeast 21, 661–670.
Sherman F (1991). Getting started with yeast. Methods Enzymol 194, 3–21.
Sidrauski C, Walter P (1997). The transmembrane kinase Ire1p is a site-specific endonuclease that initiates mRNA splicing in the unfolded protein response. Cell 90, 1031–1039.
Spear ED, Ng DT (2003). Stress tolerance of misfolded carboxypeptidase Y requires maintenance of protein trafficking and degradative pathways. Mol Biol Cell 14, 2756–2767.
Sturgill TW, Cohen A, Diefenbacher M, Trautwein M, Martin DE, Hall MN (2008). TOR1 and TOR2 have distinct locations in live cells. Eukaryot Cell 7, 1819–1830.
Swanson R, Locher M, Hochstrasser M (2001). A conserved ubiquitin ligase of the nuclear envelope/endoplasmic reticulum that functions in both ER-associated and Matalpha2 repressor degradation. Genes Dev 15, 2660–2674.
Takeda K, Cabrera M, Rohde J, Bausch D, Jensen ON, Ungermann C (2008). The vacuolar V1/V0-ATPase is involved in the release of the HOPS subunit Vps41 from vacuoles, vacuole fragmentation and fusion. FEBS Lett 582, 1558–1563.
Toulmay A, Prinz WA (2013). Direct imaging reveals stable, micrometer-scale lipid domains that segregate proteins in live cells. J Cell Biol 202, 35–44.
Travers KJ, Patil CK, Wodicka L, Lockhart DJ, Weissman JS, Walter P (2000). Functional and genomic analyses reveal an essential coordination between the unfolded protein response and ER-associated degradation. Cell 101, 249–258.
Ungermann C, Wickner W, Xu Z (1999). Vacuole acidification is required for trans-SNARE pairing, LMA1 release, and homotypic fusion. Proc Natl Acad Sci USA 96, 11194–11199.
Urban J, Soulard A, Huber A, Lippman S, Mukhopadhyay D, Deloche O, Wanke V, Anrather D, Ammerer G, Riezman H, *et al.* (2007). Sch9 is a major target of TORC1 in Saccharomyces cerevisiae. Mol Cell 26, 663–674.
Vida TA, Emr SD (1995). A new vital stain for visualizing vacuolar membrane dynamics and endocytosis in yeast. J Cell Biol 128, 779–792.
Walter P, Ron D (2011). The unfolded protein response: from stress pathway to homeostatic regulation. Science 334, 1081–1086.
Weisman LS (2003). Yeast vacuole inheritance and dynamics. Annu Rev Genet 37, 435–460.
Zhang T, Peli-Gulli MP, Yang H, De Virgilio C, Ding J (2012). Ego3 functions as a homodimer to mediate the interaction between Gtr1-Gtr2 and Ego1 in the ego complex to activate TORC1. Structure 20, 2151–2160.
Zieger M, Mayer A (2012). Yeast vacuoles fragment in an asymmetrical two-phase process with distinct protein requirements. Mol Biol Cell 23, 3438–3449.
Zoncu R, Bar-Peled L, Efeyan A, Wang S, Sancak Y, Sabatini DM (2011). mTORC1 senses lysosomal amino acids through an inside-out mechanism that requires the vacuolar H(+)-ATPase. Science 334, 678–683.